**THE EUROPEAN
PHYSICAL JOURNAL D**

Nonlinear Landau-Zener tunneling in Majorana's stellar representation

Qiuyi Guo[1,a], Haodi Liu[2], Tianji Zhou[3], Xu-Zong Chen[1], and Biao Wu[4,5,6,7]

[1] Institution of Quantum Electronics, School of Electronics Engineering & Computer Science, Peking University, Beijing 100871, P.R. China
[2] Center of Quantum Sciences and School of Physics, Northeast Normal University, Changchun 130024, P.R. China
[3] Department of Materials Science and Engineering, Rensselaer Polytechnic Institute, Troy, New York 12180, USA
[4] International Center for Quantum Materials, Peking University, Beijing 100871, P.R. China
[5] Collaborative Innovation Center of Quantum Matter, Beijing, P.R. China
[6] Wilczek Quantum Center, College of Science, Zhejiang University of Technology, Hangzhou 310014, P.R. China
[7] Synergetic Innovation Center for Quantum Effects and Applications, Hunan Normal University, Changsha 410081, P.R. China

Abstract. By representing the evolution of a quantum state with the trajectories of the stars on a Bloch sphere, the Majorana's stellar representation provides an intuitive way to understand quantum motion in a high dimensional projective Hilbert space. In this work we show that the Majorana's representation offers a very interesting and intuitive way to understand the nonlinear Landau-Zener tunneling. In particular, the breakdown of adiabaticity in this tunneling phenomenon can be understood as some of the stars never reaching the south pole. We also establish a connection between the Majorana stars in the second quantized model and the single star in the mean field model by using the reduced density matrix.

1 Introduction

Quantum motions in high dimensional Hilbert space are hard to understand intuitively and geometrically. Majorana's insight was that we can establish a geometric picture with multiple points on the Bloch sphere rather than one point on a high dimensional Hilbert space [1]. In the stellar representation established by him [1], for a spin-$n/2$ system, a quantum state is represented by n stars on the Bloch sphere [2] and its dynamics are described by the trajectories of these stars on the sphere. This representation is so intuitive that Penrose used it in his book [3] to explain to the general public the essential difference between quantum motion and classical motion.

Furthermore, Majorana's representation yields many useful insights. For example, in the Majorana's representation, geometric phase can not only be visualized as the solid angles and distances of the Majorana stars on the Bloch sphere [4–6] but also be interpreted as Aharanov-Bohm phases acquired by the stars surrounded by a flux density in the coherent state representation [7,8]. The entanglement of a symmetric n-qubit pure state can be intuitively interpreted by the relative positions of the stars [4,9–11]. It is also useful in quantum systems such as spinor boson gases [12–16], multilevel qubits [17], and Lipkin-Meshkov-Glick model [18,19].

In this work we use Majorana's representation to visualize the nonlinear Landau-Zener (LZ) tunneling [20,22,23], which has been observed experimentally with Bose-Einstein condensates (BECs) [24,25]. This nonlinear Landau-Zener tunneling can occur in a double-well BEC system, which can be described by a second quantized two-state model with N bosons. The quantum motion of such a system can be represented by the trajectories of N Majorana stars on the Bloch sphere. During the tunneling, the N stars move from the north pole to the south pole. When the interaction is small, all the stars can reach the south pole; when the interaction is strong enough, some of the stars can never reach the south pole. This corresponds to the well-known breakdown of adiabaticity in the nonlinear LZ tunneling. When the total number of bosons N is very large ($N \rightarrow \infty$), this system can be described alternatively by a mean-field theory [20,22,26]. In the mean-field description, there is only one Majorana star on the Bloch sphere. The breakdown of adiabaticity is manifested as the star in the mean-field model never reaches the south pole. The trajectories of N Majorana stars in the second quantized model (SQM) is certainly connected to the trajectory of the single star in the corresponding mean field model (MFM). This connection is established explicitly with reduced density matrix.
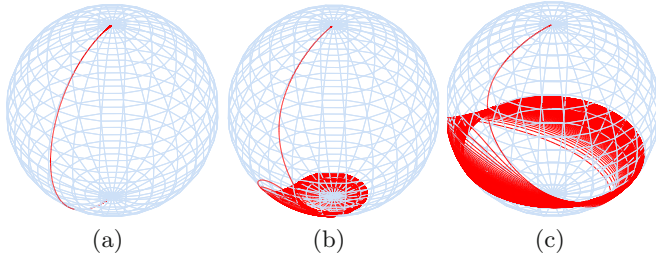
a e-mail: qyguo@pku.edu.cn

Fig. 1. Majorana representation of the mean-field model. (a) $c = 0$, (b) $c = 0.2$, (c) $c = 0.4$. Other parameters are $v = 0.2, \alpha = 0.001$.

2 Mean-field model

In this section, we focus on the MFM, which is given by the following dimensionless Schrödinger equation [22,23]

$$i\frac{\partial}{\partial t}\begin{pmatrix} a \\ b \end{pmatrix} = H(\gamma)\begin{pmatrix} a \\ b \end{pmatrix} \quad (1)$$

with

$$H(\gamma) = \begin{pmatrix} \frac{c}{2}(|b|^2 - |a|^2) + \frac{\gamma}{2} & v/2 \\ v/2 & -\frac{c}{2}(|b|^2 - |a|^2) - \frac{\gamma}{2} \end{pmatrix} \quad (2)$$

where c is the nonlinear interaction strength between bosons, γ denotes the level separation, and v is the coupling parameter between the two levels. The total probability $|a|^2 + |b|^2$ is conserved to be 1. When γ is changed at a constant rate, i.e., $\gamma = \alpha t$, tunneling occurs between the two states. This is the nonlinear LZ tunneling.

This mean-field model can be regarded as a spin-1/2 system, and its quantum state can be represented as a star on the Bloch sphere. The north pole is $(a, b) = (1, 0)$ and is denoted as $|0\rangle$ while the south pole is $(a, b) = (0, 1)$ and denoted as $|1\rangle$. A quantum state $|\Psi\rangle = a|0\rangle + b|1\rangle$ can be alternatively described by (up to an overall phase)

$$|\Psi\rangle = \cos\frac{\theta}{2}|1\rangle + \sin\frac{\theta}{2}e^{i\phi}|0\rangle, \quad (3)$$

where θ and ϕ specify the position of the star on the Bloch sphere. The population at the two states is reflected by the latitude of the star on the Bloch sphere. If the star is on the northern hemisphere, more particles are in mode a; if it is on the southern hemisphere, more particles are in mode b.

To study LZ tunneling, we start the system at the north pole and change the level bias γ with a constant sweeping rate α. In the linear situation ($c = 0$), as γ is changed from -5 to 5 with a small sweeping rate ($\alpha = 0.001$), the system moves from the north pole and reaches the south pole as shown in Figure 1a. This corresponds to the spin completely flips. If the sweeping rate is big, the star will not reach the south pole. This is the well-known LZ tunneling. As the interaction increases, the trajectory of the star becomes more interesting. At the critical point $c = v = 0.2$ and with a small sweeping rate, as

shown in Figure 1b, the star travels around the south pole for many rounds before finally reaching it. When $c = 0.4$ that is bigger than $v = 0.2$, the star will never reach the south pole and instead travel around above the south pole forever as shown in Figure 1c. This is the characteristic feature of the nonlinear LZ tunneling, that is, tunneling occurs even in the adiabatic limit [20]. In other words, the adiabaticity breaks down when the interaction is strong enough.

3 Second quantized models

The mean field model is valid only when N, the number of bosons, is large. When N is finite, the system is more accurately described by the second quantized model. The second-quantized Hamiltonian of this system can be written as:

$$\hat{H} = \frac{\gamma}{2}\left(\hat{a}_\uparrow^\dagger \hat{a}_\uparrow - \hat{a}_\downarrow^\dagger \hat{a}_\downarrow\right) + \frac{v}{2}\left(\hat{a}_\uparrow^\dagger \hat{a}_\downarrow + \hat{a}_\uparrow \hat{a}_\downarrow^\dagger\right)$$
$$- \frac{c}{4N}\left(\hat{a}_\uparrow^\dagger \hat{a}_\uparrow - \hat{a}_\downarrow^\dagger \hat{a}_\downarrow\right)^2 \quad (4)$$

where $\hat{a}_\uparrow^\dagger, \hat{a}_\uparrow$ and $\hat{a}_\downarrow^\dagger, \hat{a}_\downarrow$ are the generators and annihilators for "spin-up" (in the left well) and "spin-down" (in the right well) quantum state, respectively.

The second-quantized model can be reduced to the mean-field model (2) in the limit of $N \to \infty$. We focus on the GP state $|\Psi_{GP}\rangle = \frac{1}{\sqrt{N!}}(a\hat{a}^\dagger + b\hat{b}^\dagger)^N|vac\rangle$ [21] and compute the expectation value $\langle\hat{H}\rangle = \langle\Psi_{GP}|\hat{H}|\Psi_{GP}\rangle$. The mean-field model (2) is obtained as $H = \langle\hat{H}\rangle/N$. One can readily check that the probabilities in states a and b are $\langle\Psi_{GP}|\hat{a}^\dagger\hat{a}|\Psi_{GP}\rangle = |a|^2$ and $\langle\Psi_{GP}|\hat{b}^\dagger\hat{b}|\Psi_{GP}\rangle = |b|^2$, respectively.

As the total number of bosons N is conserved in this system, the two-mode state of the system can usually be expressed as:

$$|\Psi\rangle = \sum_{m=0}^{N} B_m|m, N-m\rangle$$
$$= \left[B_0\frac{\hat{a}_\uparrow^{\dagger N}}{\sqrt{N!}} + B_1\frac{\hat{a}_\uparrow^{\dagger N-1}\hat{a}_\downarrow^\dagger}{\sqrt{(N-1)!}} + B_2\frac{\hat{a}_\uparrow^{\dagger N-2}\hat{a}_\downarrow^{\dagger 2}}{\sqrt{(N-2)!2!}} \right. \quad (5)$$
$$\left. + \ldots + B_N\frac{\hat{a}_\downarrow^{\dagger N}}{\sqrt{N!}}\right]|\emptyset\rangle,$$

where $|m, N-m\rangle$ is a Fock state with m bosons in the left well (or in the "spin-up" state). B_m's are the coefficients and $|\emptyset\rangle$ is the vacuum state. In Majorana's stellar representation, the state has the following form:

$$|\Psi\rangle = \frac{1}{A_N}\prod_{l=0}^{N}\left[\cos(\theta_l/2)\hat{a}_\uparrow^\dagger + \sin(\theta_l/2)e^{i\phi_l}\hat{a}_\downarrow^\dagger\right]|\emptyset\rangle, \quad (6)$$

where $A_N = \sqrt{\sum_{m=0}^{N}|B_m|^2}$ is the normalization coefficient [4]. The coordinates of the Majorana stars θ_l and ϕ_l
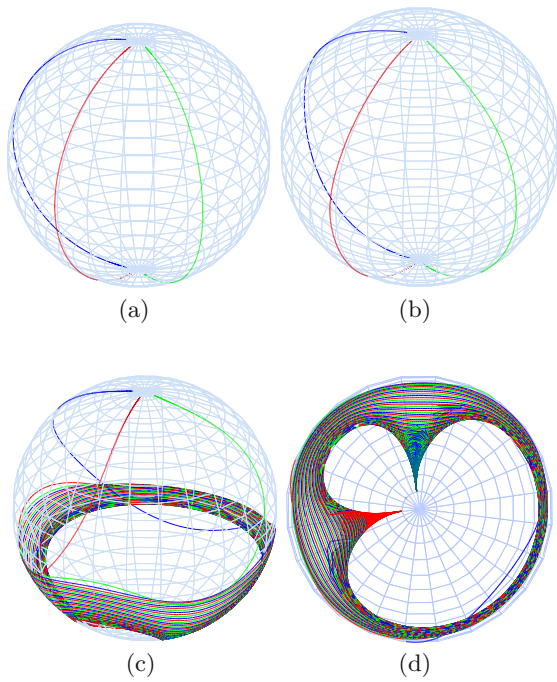
Fig. 2. Majorana representation of the second quantized model for $N = 3$. (a) $c = 0$; (b) $c = 0.2$; (c) $c = 0.6$; (d) is the bottom view from the south pole of (c). Other parameters are $v = 0.2, \alpha = 0.001$.

Fig. 3. Majorana representation of the second quantized model for $N = 4$. (a) $c = 0$; (b) $c = 0.2$; (c) $c = 0.6$; (d) is the bottom view from the south pole of (c). Other parameters are $v = 0.2, \alpha = 0.001$.

can be obtained from B_m by finding the roots of the polynomial $f(z) = \sum_{m=0}^{N} \frac{B_m}{\sqrt{(N-m)!m!}} z^m$ with the relation $z_l = \tan(\theta_l/2)e^{i\phi_l}$.

We again consider the case that the system starts at the north pole, that is, the coefficient $B_0 = 1$ and the others $B_m = 0 (m \neq 0)$. We slowly increase γ from $\gamma = -5$ to $\gamma = 5$ to see how the Majorana stars travel on the Bloch sphere. We have done calculations for big N. As there is no essential difference, our results are only plotted for small N for the sake of better illustration.

The case $N = 3$ is plotted in Figure 2. As shown in the figures, the three stars separate immediately after leaving the north pole and start to travel on different trajectories. In the simplest case where there is no interaction $c = 0$, all three stars travel straight down to the south pole as shown in Figure 2a. This situation does not change much as long as $c < v$. The critical case $c = v$ is shown in Figure 2b, which is very similar to Figure 2a. This is quite different from the mean-field picture, where there are strong oscillations before the single star reaching the south pole.

As pointed out in reference [20] and also illustrated in Figure 1c, the adiabaticity breaks down when the interaction is strong enough, that is, $c > v$. It is interesting to speculate how this effect will emerge in the picture of multiple Majorana stars. Two scenarios can happen: (i) all the stars never reach the south pole or (ii) only some of the stars never arrive at the south pole. Our calculations show that the latter is right as shown in Figure 2c.
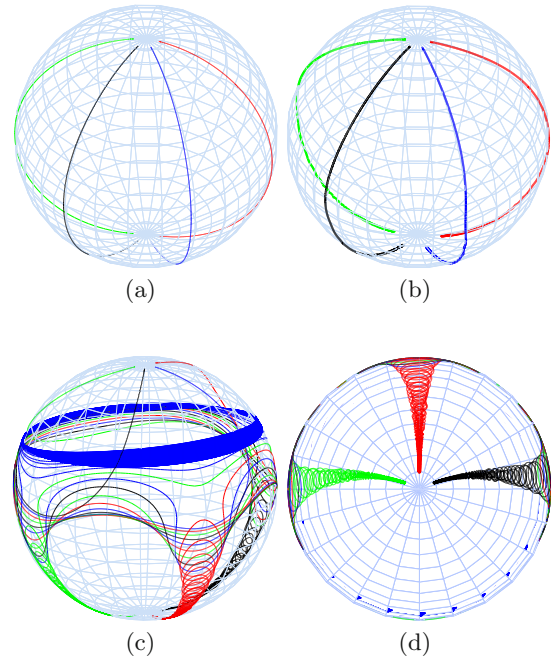
It is clear from the figure that all the stars begin to travel around latitudinally for many rounds after the departure from the north pole. However, their eventual fates are different: two of them (red and green) will arrive at the south pole while one of them never reaches the south pole. The situation is similar for $N = 4$ (see Fig. 3) and other values of N.

As we have shown above, for the second quantized model, the nonlinear LZ tunneling is now described by the motions of N Majorana stars on the Bloch sphere. This reveals a much richer picture of this interesting phenomenon. Now the question is how the motions of these N Majorana stars correspond to the motion of a single star in the mean-field description.

4 Correspondence between the mean field and the second quantized model in Majorana representation

So far we know that N bosons' dynamics can be represented by N Majorana stars moving on the Bloch sphere in SQM. On the contrary, there is only one star moving on the sphere in MFM. As the particle number $N \to \infty$, the system can perfectly described by the MFM. Therefore, we need to find a way "averaging" these Majorana stars into one star. Here, we propose a method based on density matrix to find out the relationship between these Majorana stars in SQM and the one star in MFM.

$$\begin{aligned}
\rho_r &= \mathrm{Tr}_{N-1}\rho_q \\
&= \langle\emptyset|(\hat{a}_\uparrow + \hat{a}_\downarrow)^{N-1}|\rho|(\hat{a}_\uparrow^\dagger + \hat{a}_\downarrow^\dagger)^{N-1}|\emptyset\rangle \\
&= \begin{pmatrix} \sum_{m=0}^{N-1} \frac{N-m}{N}|B_m|^2 & \sum_{m=0}^{N-1} \frac{\sqrt{(m+1)(N-m)}}{N}B_m B_{m+1}^* \\ \sum_{m=0}^{N-1} \frac{\sqrt{(m+1)(N-m)}}{N}B_{m+1}B_m^* & \sum_{m=0}^{N-1} \frac{m+1}{N}|B_{m+1}|^2 \end{pmatrix},
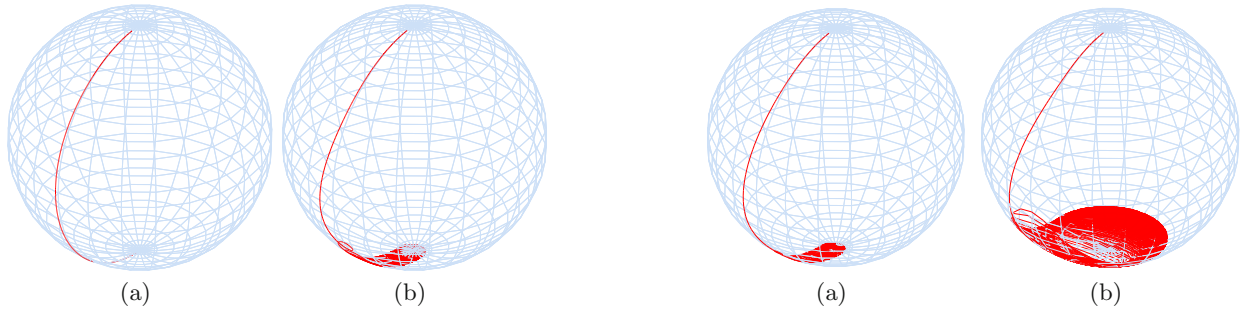\end{aligned} \tag{8}$$

(a)　　　　　　(b)

Fig. 4. The Majorana star orbit for the reduced density matrix for $N = 10$ with (a) $c = 0$; (b) $c = 0.2$. Other parameters are $v = 0.2$ and $\alpha = 0.001$.

In MFM, a state for double-well BECs can be written as $|\Psi_{\mathrm{mf}}\rangle = \cos(\frac{\theta}{2})|1\rangle + \sin(\frac{\theta}{2})e^{i\phi}|0\rangle$, and its corresponding two dimensional density matrix is:

$$\begin{aligned}
\rho_{\mathrm{mf}} &= |\Psi_{\mathrm{mf}}\rangle\langle\Psi_{\mathrm{mf}}| \\
&= \begin{pmatrix} \cos^2(\frac{\theta}{2}) & \cos^2(\frac{\theta}{2})\sin^2(\frac{\theta}{2})e^{-i\phi} \\ \cos^2(\frac{\theta}{2})\sin^2(\frac{\theta}{2})e^{i\phi} & \sin^2(\frac{\theta}{2}) \end{pmatrix}. \quad (7)
\end{aligned}$$

For a quantum state $|\Psi\rangle$ in SQM, its matrix density $\rho_q = |\Psi_q\rangle\langle\Psi_q|$ is of $(N+1)$ dimensions. When we trace out the degrees of freedom of $(N-1)$ particles, we get a 2×2 reduced matrix,

See equation (8) above.

Since the SQM can be replaced by the MFM when $N \to \infty$, the reduced density matrix ρ_r can approximate the Mean-field density matrix ρ_{mf} when N is large. The reduced density matrix ρ_r can be represented by a single Majorana star on the Bloch sphere as the mean-field density matrix ρ_{mf}. To find the spherical coordinates (θ, ϕ) of ρ_r, we use the quantum states of the SQM that we computed in the last section and compute the reduced density matrix ρ_r with equation (8). The orbits of the Majorana star of the reduced density matrix are plotted in Figures 4 and 5.

Figure 4 is for $N = 10$ with $c \leq v$. The trajectories of the Majorana star in Figure 4 are very similar to what we see in Figure 1, which is for the mean-field Majorana star: when $c = 0$, the Majorana star goes straight from the north pole to the south pole; when $c = v$, there are small oscillations before the star reaches the south pole. Note that for the multiple Majorana stars in the SQM, their trajectories do not oscillate as shown in Figures 2b and 3b.
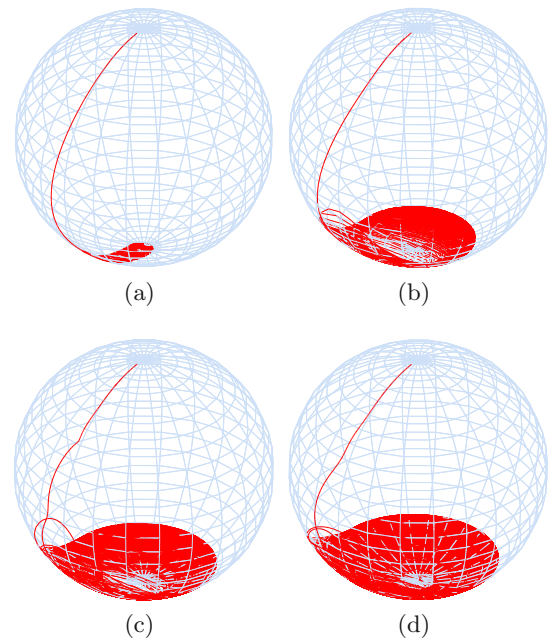

(a)　　　　　　(b)

(c)　　　　　　(d)

Fig. 5. The Majorana star orbit for the reduced density matrix for (a) $N = 3$; (b) $N = 5$; (c) $N = 10$; (d) $N = 20$. Other parameters are $c = 0.4$, $v = 0.2$, and $\alpha = 0.001$.

The case of $c > v$ is plotted in Figure 5. Just like the case of $c \leq v$, the Majorana star's orbits are very similar to their mean-field counterpart. In particular, we can see from Figure 5 that with the increase of the particle number N, the Majorana star's orbits look more similar to the mean-field trajectory shown in Figure 1c. This is just what we have expected.

5 Conclusion

In summary, we have investigated the Majorana's stellar representation of nonlinear Landau-Zener tunneling in both the mean-field model and the second-quantized model. The Majorana's representation provides a very intuitive and geometric way to understand this interesting phenomenon. We have also established the corresponding relationship between the one star in the mean-field model and the Majorana stars in the second-quantized model. It is interesting in the future to investigate the interaction between Majorana stars with this simple nonlinear Landau-Zener model.

Author contribution statement

All authors contributed equally to the paper.

References

1. E. Majorana, Nuovo Cimento **57**, 43 (1932)
2. F. Bloch, I.I. Rabi, Rev. Mod. Phys. **17**, 237 (1945)
3. R. Penrose, *The Emperor's New Mind: Concerning Computers, Minds, and the Laws of Physics* (Oxford University Press, Oxford, 1990)
4. H.D. Liu, L.B. Fu, Phys. Rev. Lett. **113**, 240403 (2014)
5. S. Tamate, K. Ogawa, M. Kitano, Phys. Rev. A **84**, 052114 (2011)
6. K. Ogawa, S. Tamate, H. Kobayashi, T. Nakanishi, M. Kitano, Phys. Rev. A **91**, 062118 (2015)
7. P. Bruno, Phys. Rev. Lett. **108**, 240402 (2012)
8. Q. Niu, Physics **5**, 65 (2012)
9. T. Bastin, S. Krins, P. Mathonet, M. Godefroid, L. Lamata, E. Solano, Phys. Rev. Lett. **103**, 070503 (2009)
10. P. Ribeiro, R. Mosseri, Phys. Rev. Lett. **106**, 180502 (2011)
11. W. Ganczarek, M. Kuś, K. Życzkowski, Phys. Rev. A **85**, 32314 (2012)
12. D. Stamper-Kurn, M. Ueda, Rev. Mod. Phys. **85**, 1191 (2013)
13. B. Lian, T.L. Ho, H. Zhai, Phys. Rev. A **85**, 051606 (2012)
14. X.L. Cui, B. Lian, T.L. Ho, B.L. Lev, H. Zhai, Phys. Rev. A **88**, 011601(R) (2013)
15. R. Barnett, D. Podolsky, G. Refael, Phys. Rev. B **80**, 024420 (2009)
16. A. Lamacraft, Phys. Rev. B **81**, 184526 (2010)
17. A.R. Usha Devi, Sudha, A.K. Rajagopal, Quantum Inf. Process. **11**, 685 (2012)
18. P. Ribeiro, J. Vidal, R. Mosseri, Phys. Rev. Lett. **99**, 050402 (2007)
19. P. Ribeiro, J. Vidal, R. Mosseri, Phys. Rev. E **78**, 021106 (2008)
20. B. Wu, Q. Niu, Phys. Rev. A **61**, 023402 (2000)
21. A.J. Leggett, Rev. Mod. Phys. **73**, 307 (2001)
22. J. Liu, B. Wu, Q. Niu, Phys. Rev. Lett. **90**, 170404 (2003)
23. B. Wu, Q. Niu, New J. Phys. **5**, 104 (2003)
24. Y.A. Chen, S.D.Huber, S. Trotzky, I. Bloch, E. Altman, Nat. Phys. **7**, 61 (2011)
25. M. Jona-Lasinio, O. Morsch, M. Cristiani, N. Malossi, J.H. Müller, E. Courtade, M. Anderlini, E. Arimondo, Phys. Rev. Lett. **91**, 230406 (2003)
26. A. Leggett, Rev. Mod. Phys. **73**, 307 (2001)